


Calcining temperature dependence on structure and dielectric properties of $\text{CaCu}_3\text{Ti}_4\text{O}_{12}$ ceramics

X. W. Wang¹  · P. B. Jia¹ · X. E. Wang¹ · B. H. Zhang¹ · L. Y. Sun¹ · Q. B. Liu¹

Received: 2 June 2016 / Accepted: 12 July 2016 / Published online: 14 July 2016
© Springer Science+Business Media New York 2016

Abstract $\text{CaCu}_3\text{Ti}_4\text{O}_{12}$ powders were obtained by calcining the precursor, which was synthesized by sol–gel process, at different temperatures, and the ceramics were obtained by dry pressing and sintering using the powders. The dependence of calcining temperature on the microstructure and dielectric properties of the ceramics was studied. The results show that the grain size of the powder grows larger with increasing calcining temperature from 700 to 1000 °C. With increasing the calcining temperature, the grain size of CCTO ceramics increases and then decreases, while the porosity exhibits an opposite trend. The ceramic, obtained by using the powders calcined at 850 °C, shows the largest grain size, and it also shows good dielectric properties with the dielectric constant of 2.61×10^4 and the dielectric loss of 0.12 at 1 kHz.

1 Introduction

Materials which show high dielectric constants (ϵ_r) accompanied by low dielectric loss ($\tan \delta$) and good temperature stability have drawn much attention due to their significant applications in energy storage devices and microelectronic devices [1–4]. In the last few years, calcium copper titanate ($\text{CaCu}_3\text{Ti}_4\text{O}_{12}$, CCTO), a kind of perovskite-like material, has gained more and more popularity because of its unusual giant dielectric constant of

about 10^4 and good stability in the 100–400 K temperature range below 1 MHz [5–7]. Therefore, CCTO has attracted considerable attention for its potential applications and nature of its dielectric properties since high dielectric constant will lead to miniaturization of electronic devices [8, 9]. A model of internal barrier layer capacitor (IBLC) has been widely used to describe the colossal dielectric constant in CCTO system [10]. However, some experimental results cannot be explained reasonably [11, 12], and a detailed explanation of the giant dielectric constant mechanism and a discussion of the influence of preparation process on the properties of samples are needed.

Most of previous works focused on the sintering method to get the well-qualified CCTO ceramics, such as microwave sintering, spark plasma sintering and rapid sintering [13–16]. But the property of CCTO powder is also the key factor to obtain high performance of CCTO ceramics, so the powder preparation method and the parameters during the process are important to ceramic microstructure and dielectric properties, and some groups have done such researches to obtain well-quality CCTO ceramics [17, 18]. CCTO powders in many researches were prepared by traditional solid state method, which is not benefit to the homogeneous of the powder. The sol–gel method, which has shown considerable advantages such as lower reaction temperatures and ultra-fine powders which are good for ceramics, is considered to be efficient to obtain CCTO ceramics with higher dielectric constant [5]. Sun et al. have reported the preparation of CCTO ceramics with dielectric constant of $1\text{--}4 \times 10^4$ and $\tan \delta$ below 0.05 (at 1 kHz and room temperature) by the sol–gel route [19]. Somsack et al. [20] have reported a modified sol–gel process for the preparation of CCTO ceramics with lower $\tan \delta$ of 0.02 and a dielectric

✉ X. W. Wang
xwwang2000@163.com

¹ Laboratory of Functional Materials, College of Physics and Materials Science, Henan Normal University, and Henan Key Laboratory of Photovoltaic Materials, Xinxiang 453007, China

constant of 9.5×10^3 at 1 kHz at room temperature. Also, the calcining temperature is an important factor for the powder properties which will affect the ceramics [17], but there are a limited number of literatures reporting the effects of calcining temperature of CCTO powders prepared by the sol–gel method on the microstructure and properties of ceramics. In this work, CCTO powders were prepared via a sol–gel method followed by calcining at different temperatures. The obtained CCTO powders with perovskite-like structure were used to fabricate CCTO ceramics. The dependence of calcining temperature of CCTO powders on the microstructure and properties of ceramics was investigated.

2 Experimental procedure

$\text{Ca}(\text{COOH})_2 \cdot 4\text{H}_2\text{O}$ (99 %), $\text{Cu}(\text{NO}_3)_2 \cdot 3\text{H}_2\text{O}$ (99 %) and $\text{Ti}(\text{OC}_4\text{H}_9)_4$ (≥ 98.0 %) were used as raw materials. Firstly, an appropriate amount of $\text{Cu}(\text{NO}_3)_2 \cdot 3\text{H}_2\text{O}$ was dissolved in ethanol to form solution 1, and calculated amount of $\text{Ca}(\text{COOH})_2 \cdot 4\text{H}_2\text{O}$ was dissolved in distilled water to form solution 2. Meanwhile, $\text{Ti}(\text{OC}_4\text{H}_9)_4$ was dissolved into ethanol, and CH_3COOH was added into the solution immediately under vigorously stirring to form solution 3. Secondly, solution 1 was added into solution 3 slowly under stirring followed by stirring for 20 min, then solution 2 was added into the preceding mixed solution under stirring, and the mixed solutions were then stirred for 1 h at room temperature after the pH value was adjusted to 3. Then, the mixture was dried at 85 °C for 15 h and 125 °C for 8 h in a drying oven, followed by drying at 350 °C for 3 h in a muffle furnace to form the precursor. Finally, different CCTO powders were obtained by calcining the precursor at 700, 750, 800, 850, 900 and 1000 °C for 10 h, respectively. The as-prepared different CCTO powders were pressed into different pellets with the diameter of 10 mm under the pressure of 200 MPa. Different CCTO ceramics were obtained by sintering the different pellets at 1050 °C for 20 h.

The crystal structures of the powder and ceramic samples were identified by X-ray diffraction (XRD, Bruker D8 discover) at 40 kV and 40 mA. The microstructures of the samples were observed by field emission scanning electron microscopy (FE-SEM, Zeiss SUPRA 40). For measuring the dielectric properties, both sides of the ceramic samples were coated by silver paste and fired at 680 °C to form silver electrodes. Dielectric properties were measured by LCR meter (Tonghui, TH2826) at room temperature. Temperature dependence of the dielectric properties for CCTO ceramics was conducted by putting samples in oil bath.

3 Results and discussion

Figure 1 shows the XRD patterns of the CCTO powders obtained by calcining at different temperatures. As shown in Fig. 1, CCTO phase appear in all the samples, and diffraction peaks are indexed as the perovskite phase. It can be seen clearly that the main peaks of powders obtained by calcining at 700 °C are assigned to CCTO phase, indicating the temperature has reached the CCTO formation temperature, and the crystalline temperature in the sol–gel method has reduced 100 °C compared with that in the traditional solid state method [1, 3, 21–23]. In addition, secondary phases of CaTiO_3 , CuO and TiO_2 , are also detected in powders obtained by calcining at 700 °C. With increasing the calcination temperature, the diffraction peak intensities of CCTO phase are gradually increased. While the peak intensities of the TiO_2 , CuO and CaTiO_3 impurities become strong in the calcination temperature range of 700–800 °C and then become weak when the temperature is higher than 800 °C.

Figure 2 reveals the SEM images of CCTO powders obtained by calcining at 700–1000 °C for 10 h. As observed in Fig. 2a, there are lots of ultrafine particles in the powder obtained by calcining at 700 °C. The grains grow larger with increasing the calcination temperature to 750 °C according to Fig. 2b. Higher than 800 °C, some grains begin to grow larger abnormally in the matrix of small grains, as seen in Fig. 2c. Figure 2d shows that the grains agglomerate together obviously when calcination temperature reaches to 850 °C, and it could be attributed to the forming of liquid in the calcining process. Figure 2e, f show dense grains and clear grain boundaries in samples obtained by calcining at 900 and 1000 °C, indicating that

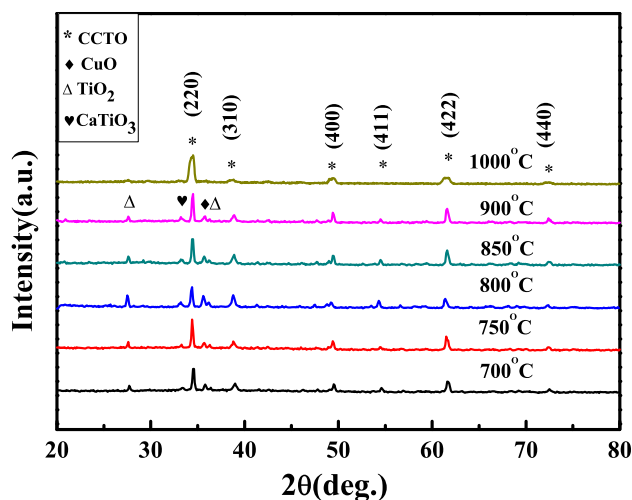


Fig. 1 XRD patterns of CCTO powders obtained by calcining at 700–1000 °C

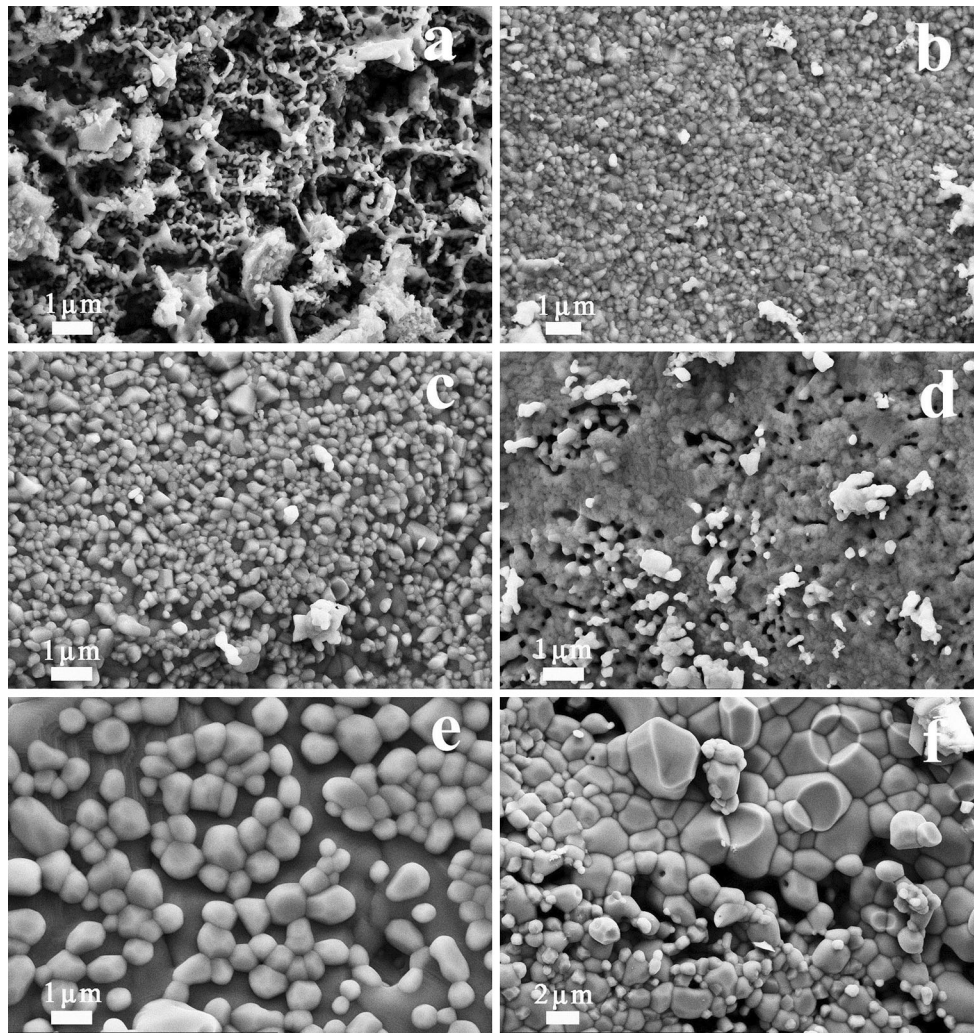


Fig. 2 SEM images of CCTO powders obtained by calcining at **a** 700 °C, **b** 750 °C, **c** 800 °C, **d** 850 °C, **e** 900 °C and **f** 1000 °C

the calcination temperature is too high and that sintering process has begun in the calcining process.

Figure 3 reveals the XRD patterns of the ceramic specimens sintered at 1050 °C for 20 h from powders obtained by calcining at 700–1000 °C. It is noted that a single perovskite structure was observed in all the sintered ceramics and no second phase could be detected in the sintered samples. According to the XRD patterns of powders shown in Fig. 1, we can draw a conclusion that all other phases, such as CaTiO_3 , CuO and TiO_2 , are transformed into CCTO during the sintering process.

Figure 4 shows SEM images of CCTO ceramics prepared at 1050 °C for 20 h from CCTO powders obtained by calcining at different temperatures for 10 h. With increasing the calcining temperature, the grain size of the samples firstly increases and then decreases, while the porosity exhibits an opposite variation trend. As is depicted in Fig. 4a, b, ceramics prepared from powders obtained by

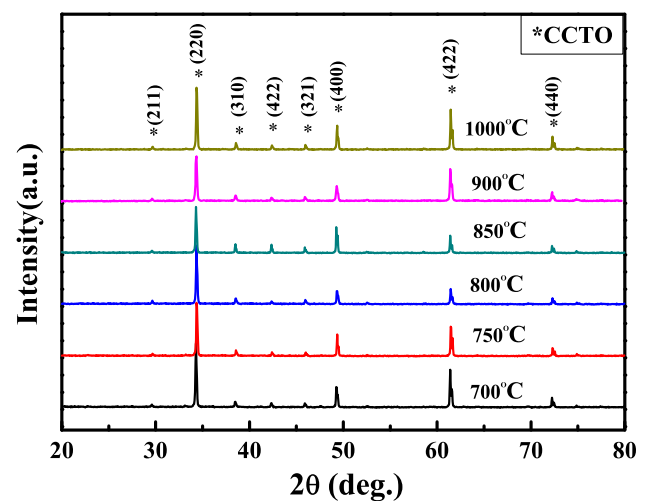


Fig. 3 XRD patterns of CCTO ceramics prepared from powders obtained by calcining at 700–1000 °C

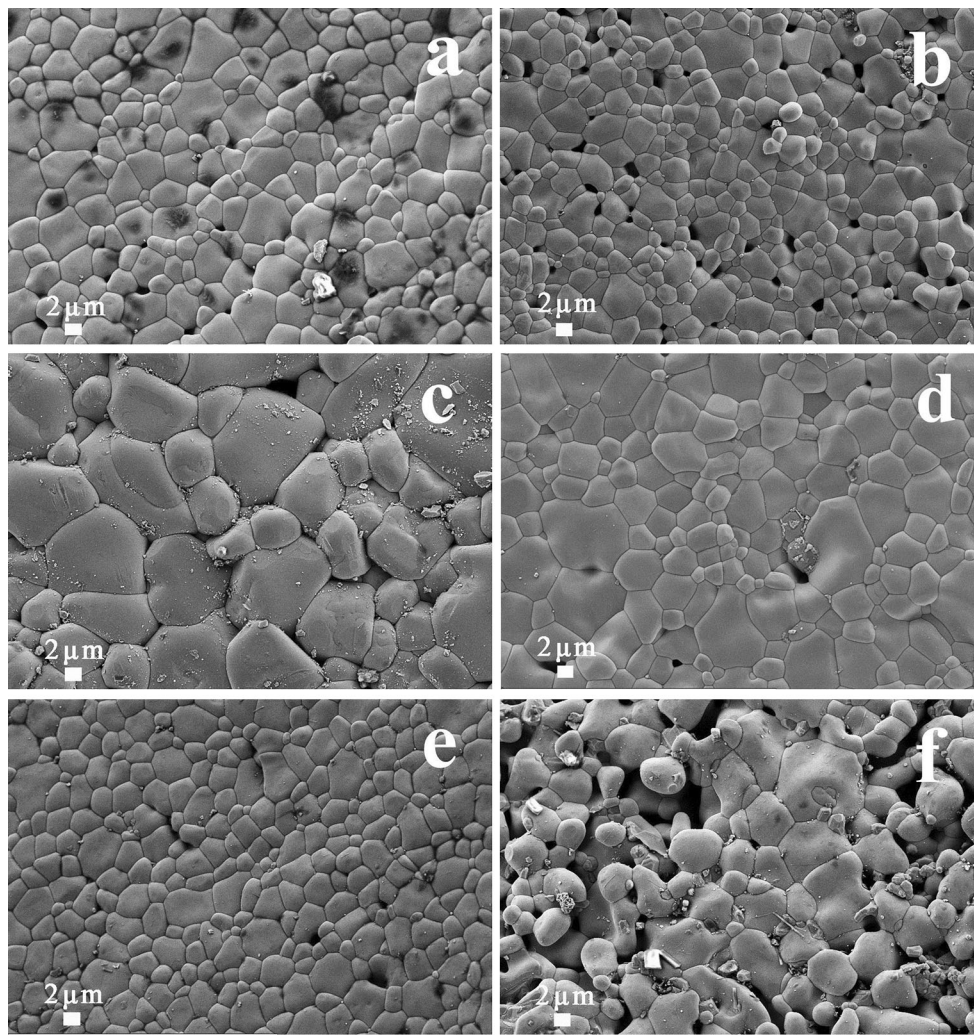


Fig. 4 SEM images of CCTO ceramics obtained from powders obtained by calcining at **a** 700 °C, **b** 750 °C, **c** 800 °C, **d** 850 °C, **e** 900 °C and **f** 1000 °C

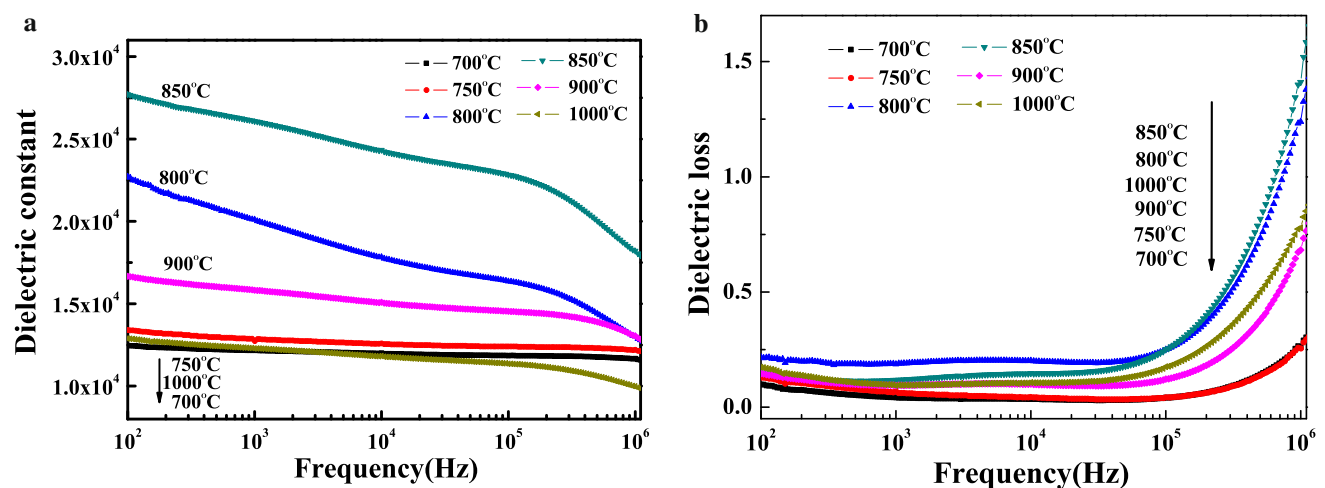
calcining at 700 and 750 °C show a relatively homogeneous microstructure with clear grain boundaries and small grain size with 2–6 μm. Figure 4c, d show the surface of ceramics prepared from powders obtained by calcining at 800 and 850 °C, a number of grains grow abnormally, and the size of the largest abnormal grain exceeded 10 μm for ceramics prepared from powders obtained by calcining at 800 and 850 °C. However, as illustrated in Fig. 4e, the grain size of ceramics prepared from powders obtained by calcining at 900 °C becomes small again. The microstructure becomes inhomogeneous with high porosity for ceramics from powders obtained by calcining at 1000 °C. The abnormal grain growth in ceramics obtained from powders prepared by calcining at 800 and 850 °C could be attributed to those larger grains in the matrix of small grains, which have higher chemical activity [5], and the small grain will disappear in sintering process due to the secondary recrystallization. For powders with high

calcining temperature of 900 and 1000 °C, the serious aggregation or sintering phenomena during calcining process is harmful to the following sintering process. Thus the powder calcining temperature has a great influence on ceramic microstructures. Densities of ceramic samples are listed in Table 1, and the density of ceramic increases and then decreases with the increasing of calcining temperature. The density of the CCTO ceramics obtained from powder calcined at 850 °C reaches to a maximum value of 4.43 g/cm³. The variation of density is consistent with the variation of CCTO ceramic microstructure.

For ceramics sintered at 1050 °C for 20 h using different powders obtained by calcining at different temperatures, the dependence of dielectric constant and dielectric loss $\tan \delta$ on frequency at room temperature is shown in Fig. 5a, b. It was seen that calcining temperatures have obvious effects on the dielectric properties of CCTO ceramics. According to Fig. 5a, the dielectric constant

Table 1 Densities and dielectric properties of CCTO ceramics prepared from powders obtained by calcining at 700–1000 °C

Calculating temperature (°C)	Density (g/Cm ³)	Dielectric properties					
		1 kHz		10 kHz		100 kHz	
		ϵ' ($\times 10^4$)	$\tan \delta$	ϵ' ($\times 10^4$)	$\tan \delta$	ϵ' ($\times 10^4$)	$\tan \delta$
700	4.32	1.22	0.04	1.20	0.04	1.19	0.04
750	4.38	1.27	0.07	1.26	0.04	1.24	0.04
800	4.38	2.01	0.19	1.78	0.20	1.64	0.25
850	4.43	2.61	0.12	2.41	0.15	2.28	0.25
900	4.36	1.59	0.09	1.51	0.10	1.45	0.12
1000	4.02	1.23	0.09	1.18	0.11	1.14	0.18

**Fig. 5** Frequency dependence of **a** dielectric constant and **b** dielectric loss measured at room temperature of CCTO ceramics prepared from powders obtained by calcining at 700–1000 °C

decreases with increasing measurement frequency and knee points were observed at around 10^5 Hz. All ceramics exhibit giant dielectric constant and the value of dielectric constant for all samples are higher than 10^4 over a wide frequency range from 10^2 to 10^6 Hz. The dielectric constant of ceramics increase and then decrease with increasing the calcining temperature of powders, and the dielectric constant of sample ceramic prepared from powders obtained by calcining at 850 °C reaches the maximum value of 2.61×10^4 (1 kHz), which is about 2 times higher than that of the samples whose powders are obtained by calcining at 700, 750, 900 and 1000 °C. The dielectric constant is comparable with the reported results [4, 15, 24, 25]. As shown in Fig. 5b, the dielectric loss $\tan \delta$ of all CCTO ceramics begins to increase quickly at around 10^5 Hz, corresponding to the knee points of dielectric constant in Fig. 5a, and this can be explained by the Debye relaxation [26, 27]. As shown in Fig. 5b and Table 1, ceramics with relatively homogeneous

microstructure show low dielectric loss, and the ceramics obtained from powders whose calcining temperature are 700 and 750 °C show the lowest dielectric loss of about 0.04 in a wide frequency range. Meanwhile, the ceramics with abnormal grain growth show higher dielectric loss, and the ceramics prepared from powders with the calcining temperatures of 850 °C show a slightly lower dielectric loss ($\tan \delta = 0.12$ at 1 kHz) than that of ceramics prepared from powders obtained by calcining at 800 °C in a wide frequency range. The dielectric properties are sensitive to the calcining temperature of powders, which leads to different microstructures of ceramics, and the dielectric properties were thought to be mainly dependent on the grain size and the thickness of the grain boundary layer. The large grain size leads to giant dielectric constant together with high dielectric loss.

Figure 6a demonstrates the temperature dependence of the dielectric constant (ϵ') and dielectric loss for CCTO ceramic obtained from powders prepared by calcining at

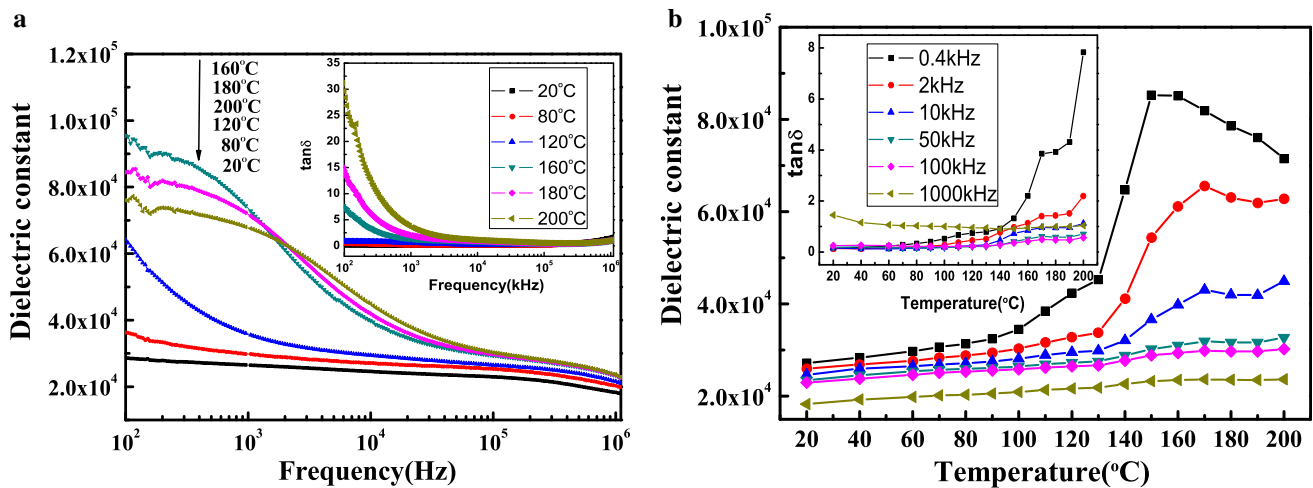


Fig. 6 **a** Temperature and **b** frequency dependence of dielectric constant and dielectric loss (*insets*) for CCTO ceramic prepared from powders obtained by calcining at 850 °C

850 °C for 10 h. The sample shows both high dielectric constant and low dielectric loss in the measured temperature range from 20 °C up to 200 °C. Dielectric constant is nearly independent on measuring temperature at high frequency, while it increases rapidly with increasing measurement temperature at low frequency, as illustrated in Fig. 6a. The increasing of dielectric constant with measurement temperature could be attributed to the variation of dielectric loss, which is shown in insets of Fig. 6a. Figure 6b reveals frequency dependence of dielectric constant and dielectric loss for CCTO ceramic prepared from powders obtained by calcining at 850 °C for 10 h between 100 Hz and 1 MHz at different measuring temperatures. A plateau region of the dielectric constant at low frequency can be observed in the dielectric spectra measured at higher temperature than 160 °C, and the dielectric loss corresponding to the plateau region of the dielectric constant at low frequency is also relatively higher than that of other frequency region, which is according to the previous work [19]. Behind the plateau region, the dielectric constant decreases rapidly to another plateau region at higher frequencies in the dielectric spectra measured at higher temperature than 160 °C, and this relaxation behavior can be described by Debye theory. With decreasing the measuring temperature, the plateau region disappears slowly and the frequency corresponding to the rapid decrease of dielectric constant changes to low frequency slowly.

4 Conclusions

$\text{CaCu}_3\text{Ti}_4\text{O}_{12}$ powders were obtained by sol–gel process followed by calcining at different temperatures from 700 to 1000 °C, and the ceramics were obtained by sintering

green pellets using the powders at 1050 °C for 20 h. With increasing the calcining temperature, the grain size of CCTO ceramics increases and then decreases, while the porosity exhibits an opposite trend. The ceramic, obtained by using the powders prepared by calcining at 850 °C, shows abnormal grain growth, leading to large grain size in the ceramic, and it also shows good dielectric properties with the dielectric constant of 2.61×10^4 and the dielectric loss of 0.12 at 1 kHz. While the ceramics obtained from powders with the calcining temperatures of 700 and 750 °C, show relatively homogeneous microstructure, and they also show good dielectric properties with the dielectric constant of about 10^4 and dielectric loss of about 0.04 in a wide frequency range.

Acknowledgments This work has been supported by the National Natural Science Foundation of China (Nos. 51402091, 11304082 and 11404102), the scientific research foundation for new introduced doctors in Henan Normal University (No. 11114), and the National University Student Innovation Program (201410476037).

References

- B.A. Bender, M.J. Pan, The effect of processing on the giant dielectric properties of $\text{CaCu}_3\text{Ti}_4\text{O}_{12}$. *Mater. Sci. Eng. B* **117**(3), 339–347 (2005). doi:10.1016/j.mseb.2004.11.019
- X. Fang, X. Liu, Z.-K. Cui, J. Qian, J. Pan, X. Li, Q. Zhuang, Preparation and properties of thermostable well-functionalized graphene oxide/polyimide composite films with high dielectric constant, low dielectric loss and high strength via in situ polymerization. *J. Mater. Chem. A* **3**(18), 10005–10012 (2015). doi:10.1039/c5ta00943j
- G. Li, Z. Chen, X. Sun, L. Liu, L. Fang, B. Elouadi, Electrical properties of $\text{AC}_3\text{B}_4\text{O}_{12}$ -type perovskite ceramics with different cation vacancies. *Mater. Res. Bull.* **65**, 260–265 (2015). doi:10.1016/j.materresbull.2015.02.012

4. D. Xu, K. He, R. Yu, X. Sun, Y. Yang, H. Xu, H. Yuan, J. Ma, High dielectric permittivity and low dielectric loss in sol–gel derived Zn doped $\text{CaCu}_3\text{Ti}_4\text{O}_{12}$ thin films. *Mater. Chem. Phys.* **153**, 229–235 (2015). doi:[10.1016/j.matchemphys.2015.01.007](https://doi.org/10.1016/j.matchemphys.2015.01.007)
5. Z. Liu, G. Jiao, X. Chao, Z. Yang, Preparation, microstructure, and improved dielectric and nonlinear electrical properties of $\text{Na}_{1/2}\text{La}_{1/2}\text{Cu}_3\text{Ti}_4\text{O}_{12}$ ceramics by sol–gel method. *Mater. Res. Bull.* **48**(11), 4877–4883 (2013). doi:[10.1016/j.materresbull.2013.06.056](https://doi.org/10.1016/j.materresbull.2013.06.056)
6. B. Zhu, Z. Wang, Y. Zhang, Z. Yu, J. Shi, R. Xiong, Low temperature fabrication of the giant dielectric material $\text{CaCu}_3\text{Ti}_4\text{O}_{12}$ by oxalate coprecipitation method. *Mater. Chem. Phys.* **113**(2–3), 746–748 (2009). doi:[10.1016/j.matchemphys.2008.08.037](https://doi.org/10.1016/j.matchemphys.2008.08.037)
7. M. Li, X.L. Chen, D.F. Zhang, Q. Liu, C.X. Li, The effect of grain boundary resistance on the dielectric response of $\text{CaCu}_3\text{Ti}_4\text{O}_{12}$. *Ceram. Int.* **41**(10), 14854–14859 (2015). doi:[10.1016/j.ceramint.2015.08.019](https://doi.org/10.1016/j.ceramint.2015.08.019)
8. C.R. Foschini, R. Tararam, A.Z. Simões, L.S. Rocha, C.O.P. Santos, E. Longo, J.A. Varela, Rietveld analysis of $\text{CaCu}_3\text{Ti}_4\text{O}_{12}$ thin films obtained by RF-sputtering. *J. Mater. Sci. Mater. Electron.* **27**(3), 2175–2182 (2015). doi:[10.1007/s10854-015-4084-y](https://doi.org/10.1007/s10854-015-4084-y)
9. M. Xiao, K. Wang, X. Chenyang, S. Xie, Nonlinear current–voltage behavior of $\text{CaCu}_3\text{Ti}_4\text{O}_{12}$ thin films derived from sol–gel method. *J. Mater. Sci. Mater. Electron.* **25**(6), 2710–2715 (2014). doi:[10.1007/s10854-014-1933-z](https://doi.org/10.1007/s10854-014-1933-z)
10. J. Zhao, J. Liu, G. Ma, Preparation, characterization and dielectric properties of $\text{CaCu}_3\text{Ti}_4\text{O}_{12}$ ceramics. *Ceram. Int.* **38**(2), 1221–1225 (2012). doi:[10.1016/j.ceramint.2011.08.052](https://doi.org/10.1016/j.ceramint.2011.08.052)
11. S. De Almeida-Didry, C. Autret, C. Honstette, A. Lucas, F. Pacreau, F. Gervais, Capacitance scaling of grain boundaries with colossal permittivity of $\text{CaCu}_3\text{Ti}_4\text{O}_{12}$ -based materials. *Solid State Sci.* **42**, 25–29 (2015). doi:[10.1016/j.solidstatesciences.2015.03.004](https://doi.org/10.1016/j.solidstatesciences.2015.03.004)
12. J. Li, A.W. Sleight, M.A. Subramanian, Evidence for internal resistive barriers in a crystal of the giant dielectric constant material: $\text{CaCu}_3\text{Ti}_4\text{O}_{12}$. *Solid State Commun.* **135**(4), 260–262 (2005). doi:[10.1016/j.ssc.2005.04.028](https://doi.org/10.1016/j.ssc.2005.04.028)
13. R. Kumar, M. Zulfeqar, T.D. Senguttuvan, Structural and impedance spectroscopic studies of spark plasma sintered $\text{CaCu}_3\text{Ti}_4\text{O}_{12}$ dielectric ceramics: an evidence of internal resistive barrier effect. *J. Mater. Sci. Mater. Electron.* **27**(5), 5233–5237 (2016). doi:[10.1007/s10854-016-4418-4](https://doi.org/10.1007/s10854-016-4418-4)
14. R. Kumar, M. Zulfeqar, T.D. Senguttuvan, Dielectric properties of microwave flash combustion derived and spark plasma sintered $\text{CaCu}_3\text{Ti}_4\text{O}_{12}$ ceramic: role of reduction in grain boundary activation energy. *J. Mater. Sci.: Mater. Electron.* **26**(9), 6718–6722 (2015). doi:[10.1007/s10854-015-3275-x](https://doi.org/10.1007/s10854-015-3275-x)
15. R. Kumar, M. Zulfeqar, V.N. Singh, J.S. Tawale, T.D. Senguttuvan, Microwave sintering of dielectric $\text{CaCu}_3\text{Ti}_4\text{O}_{12}$: an interfacial conductance and dipole relaxation effect. *J. Alloy. Compd.* **541**, 428–432 (2012). doi:[10.1016/j.jallcom.2012.07.052](https://doi.org/10.1016/j.jallcom.2012.07.052)
16. J.Q. Wang, X. Huang, X.H. Zheng, D.P. Tang, Structure and electric properties of $\text{CaCu}_3\text{Ti}_4\text{O}_{12}$ ceramics prepared by rapid sintering. *J. Mater. Sci. Mater. Electron.* **27**(2), 1345–1349 (2015). doi:[10.1007/s10854-015-3895-1](https://doi.org/10.1007/s10854-015-3895-1)
17. T. Li, R. Xue, J. Hao, Y. Xue, Z. Chen, The effect of calcining temperatures on the phase purity and electric properties of $\text{CaCu}_3\text{Ti}_4\text{O}_{12}$ ceramics. *J. Alloy. Compd.* **509**(3), 1025–1028 (2011). doi:[10.1016/j.jallcom.2010.09.163](https://doi.org/10.1016/j.jallcom.2010.09.163)
18. X. Chao, P. Wu, Y. Zhao, P. Liang, Z. Yang, Effect of $\text{CaCu}_3\text{Ti}_4\text{O}_{12}$ powders prepared by the different synthetic methods on dielectric properties of $\text{CaCu}_3\text{Ti}_4\text{O}_{12}$ /polyvinylidene fluoride composites. *J. Mater. Sci. Mater. Electron.* **26**(5), 3044–3051 (2015). doi:[10.1007/s10854-015-2795-8](https://doi.org/10.1007/s10854-015-2795-8)
19. L. Sun, Z. Wang, Y. Shi, E. Cao, Y. Zhang, H. Peng, L. Ju, Sol–gel synthesized pure $\text{CaCu}_3\text{Ti}_4\text{O}_{12}$ with very low dielectric loss and high dielectric constant. *Ceram. Int.* **41**(10), 13486–13492 (2015). doi:[10.1016/j.ceramint.2015.07.140](https://doi.org/10.1016/j.ceramint.2015.07.140)
20. S. Vangchangyia, E. Swatsitang, P. Thongbai, S. Pinitsoontorn, T. Yamwong, S. Maensiri, V. Amornkitbamrung, P. Chindaprasirt, J. Hu, Very low loss tangent and high dielectric permittivity in pure- $\text{CaCu}_3\text{Ti}_4\text{O}_{12}$ ceramics prepared by a modified sol-gel process. *J. Am. Ceram. Soc.* **95**(5), 1497–1500 (2012). doi:[10.1111/j.1551-2916.2012.05147.x](https://doi.org/10.1111/j.1551-2916.2012.05147.x)
21. R. Jia, X. Zhao, J. Li, X. Tang, Colossal breakdown electric field and dielectric response of Al-doped $\text{CaCu}_3\text{Ti}_4\text{O}_{12}$ ceramics. *Mater. Sci. Eng. B* **185**, 79–85 (2014). doi:[10.1016/j.mseb.2014.02.015](https://doi.org/10.1016/j.mseb.2014.02.015)
22. L. Singh, U.S. Rai, K.D. Mandal, B.C. Sin, Lee H-i, H. Chung, Y. Lee, Comparative dielectric studies of nanostructured BaTiO_3 , $\text{CaCu}_3\text{Ti}_4\text{O}_{12}$ and $0.5\text{BaTiO}_3\text{-}0.5\text{CaCu}_3\text{Ti}_4\text{O}_{12}$ nano-composites synthesized by modified sol–gel and solid state methods. *Mater. Charact.* **96**, 54–62 (2014). doi:[10.1016/j.matchar.2014.07.019](https://doi.org/10.1016/j.matchar.2014.07.019)
23. L. Singh, U.S. Rai, K.D. Mandal, N.B. Singh, Progress in the growth of $\text{CaCu}_3\text{Ti}_4\text{O}_{12}$ and related functional dielectric perovskites. *Prog. Cryst. Growth Charact. Mater.* **60**(2), 15–62 (2014). doi:[10.1016/j.pcrysgrow.2014.04.001](https://doi.org/10.1016/j.pcrysgrow.2014.04.001)
24. H.E. Kim, S.-M. Choi, Y.-W. Hong, S.-I. Yoo, Improved dielectric properties of the $\text{CaCu}_3\text{Ti}_4\text{O}_{12}$ composites using BaTiO_3 -coated powder as precursor. *J. Alloy. Compd.* **610**, 594–599 (2014). doi:[10.1016/j.jallcom.2014.04.215](https://doi.org/10.1016/j.jallcom.2014.04.215)
25. J. Boonlakhorn, P. Kidkhunthod, P. Thongbai, A novel approach to achieve high dielectric permittivity and low loss tangent in $\text{CaCu}_3\text{Ti}_4\text{O}_{12}$ ceramics by co-doping with Sm^{3+} and Mg^{2+} ions. *J. Eur. Ceram. Soc.* **35**(13), 3521–3528 (2015). doi:[10.1016/j.jeurceramsoc.2015.06.008](https://doi.org/10.1016/j.jeurceramsoc.2015.06.008)
26. L. Liu, H. Fan, P. Fang, L. Jin, Electrical heterogeneity in $\text{CaCu}_3\text{Ti}_4\text{O}_{12}$ ceramics fabricated by sol–gel method. *Solid State Commun.* **142**(10), 573–576 (2007). doi:[10.1016/j.ssc.2007.04.005](https://doi.org/10.1016/j.ssc.2007.04.005)
27. T. Fang, L. Mei, H. Ho, Effects of Cu stoichiometry on the microstructures, barrier-layer structures, electrical conduction, dielectric responses, and stability of $\text{CaCu}_3\text{Ti}_4\text{O}_{12}$. *Acta Mater.* **54**(10), 2867–2875 (2006). doi:[10.1016/j.actamat.2006.02.037](https://doi.org/10.1016/j.actamat.2006.02.037)